ELECTRON BACK-SCATTERED DIFFRACTION ANALYSIS OF A REFRACTORY INCLUSION AND ITS WARK-LOVERING RIMS. P. Mane[1,2], S. Wallace[3], T. J. Zega[1], M. Wadhwa[2], and P. M. Wallace[1]. [1]Lunar and Planetary Laboratory, University of Arizona, Tucson, AZ 85721-0092. (Email: pmane@lpl.arizona.edu), [2]Center for Meteorite Studies, School of Earth and Space Exploration, Arizona State University, Tempe, AZ 85782-6004. [3]EDAX, Ametek, Materials Analysis Division, 91 McKee Drive, Mahwah, NJ 07430.

Introduction: Relative and absolute dating techniques indicate that calcium-aluminum-rich inclusions (CAIs) are the earliest formed solids in the Solar System [1, 2]. The refractory mineral phases in CAIs are predicted to have condensed at high temperatures (starting at ~1750 K) [3]. Many CAIs are surrounded by a sequence of seemingly mono- or bi- mineralic layers, termed as Wark-Lovering (WL) rims [4], which were described as early Solar System stratigraphy [4]. The WL rims show a general mineralogical sequence of the innermost spinel-perovskite-hibonite layer, followed by melilite-anorthite, Al-rich clinopyroxene and the outermost forsterite layer [4, 5]. Alteration phases such as nepheline, anorthite, sodalite, grossular and wollastonite have also been reported in the rim sequences [6-7]. Incomplete WL rims around broken CAIs and absence of rims around other chondritic components such as chondrules, suggest restricted spatial or temporal conditions of rim formation in the solar nebula. The ^{26}Al-^{26}Mg relative dating of the WL rims shows a time of formation varying from 0 to ~2.5 Ma after CAI formation [8-11]. Various mechanisms have been proposed to explain the formation of WL rims, including: 1) condensation and subsequent accretion on the CAI [5, 12-14]; 2) crystallization from a melt, via flash-heating mechanisms [15]; 3) formation as evaporation residues [16]; and 4) growth of layers as a result of chemical gradients set up during alteration of the interior of the inclusion, in nebular settings [7, 17]. Different mineral layers of WL rims were likely formed and affected by a combination of these processes. Understanding the processes and timescales involved in WL rim formation through detailed petrographic, geochemical and isotopic analyses is important, as this can provide better constraints on the environment and conditions in the early Solar System. However, since the width of these individual layers is less than a few microns (< 15-20 μm), their textural, geochemical and isotopic characterization can be a significant analytical challenge.

In order to determine formation mechanism of CAIs and their WL rims, we analyzed a coarse-grained inclusions (CAI-1) from the CV3 chondrite Northwest Africa (NWA) 8323 using electron backscattered diffraction (EBSD). This study is part of a broader effort to understand the detailed microstructures of CAIs and gain new insight into their origins [5, 18].

Sample Description and Previous Work: NWA 8323 is an oxidized CV3 chondrite that shows a low shock grade and minimal weathering effects [19]. CAI-1 is a coarse-grained type-B inclusion containing melilite, spinel, Ti-rich pyroxene, and anorthite. The WL rim sequence in CAI-1 consists of innermost anorthite, intermediate spinel, and outermost pyroxene layers; in some regions the rim sequence shows Fe-rich spinel grains and a glassy layer. The relative ^{26}Al-^{26}Mg ages have been reported for this CAI. The relative time between formation of CAI-1 interior and its WL rim is $2.2^{+0.7}_{-0.4}$ Ma [11]. In terms of Δ^{17}O, phases in this CAI range from the CAI end-member (Δ^{17}O = -25‰) up to the terrestrial value (Δ^{17}O = 0‰). [11].

Methods: We investigated CAI-1 using a JEOL JXA-8530F electron microprobe at Arizona State University to obtain backscattered electron (BSE) images of selected regions. We further investigated these regions using the FEI Helios NanoLAB 660 focused-ion-beam scanning electron microscope (FIB-SEM), equipped with an EDAX energy dispersive X-ray spectrometer (EDS) and EBSD detector, located at the Lunar and Planetary Laboratory, University of Arizona.

Results and Discussions: The EBSD map of the interior of CAI-1 shows melilite grains with triple junctions and random crystal orientation (Fig. 1A , B, and C), suggesting equilibrium conditions during melilite formation. A single anorthite grain analyzed in the region of interest shows twin lamellae (Fig.1C and D). Plagiclase twinning is common in terrestrial rocks, and it has been previously observed in TEM analyses of anorthite from coarse-grained Allende inclusions [20]. Spinel grains in this CAI region show some clusters, however, the grains in these clusters show random orientations, in contrast to the pyroxene clusters reported in WL rims previously by [5]. The misorientation map of all three mineral phases analyzed here do not show significant strain and deformation, suggesting that they are minimally affected by secondary processes. Continued examination of this CAI using EBSD and transmission electron microscopy (TEM) techniques will reveal more microstructural details to understand the formation mechanisms of this inclusion and its WL rims.

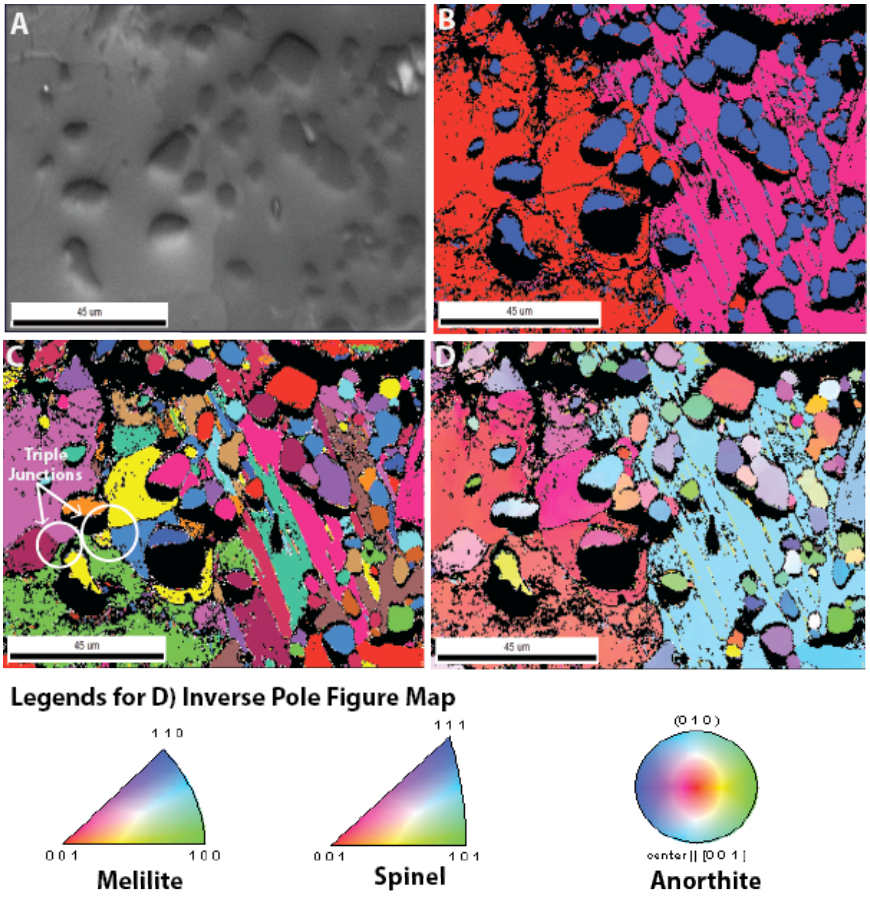

Figure 1: A) Electron back-scattered image of the interior of CAI-1. B) Mineral phase map of the same region as A, where red region is melilite, blue shows spinel and pink shows anorthite. C) Unique grain color map, showing different grain clusters of melilite, spinels and a single twinned crystal of anorthite. D) Inverse pole figure map, where the crystallographic orientations for each mineral phase (Melilite, spinel and anorthite) is shown in the legend.

References: [1] Bouvier A. et al. (2011) *GCA*, 75(18), 5310-5323. [2] Connelly J. N. et al., (2012) *Science*, 338(6107), 651-655. [3] Grossman L. (1972) *GCA*, 36(5), 597-619. [4] Wark D. A. and Lovering J. F. (1977) *LPSC VII*, 95-112. [5] Bolser D. et al. (2016) *MAPS*, 51(4), 743-756. [6] Macpherson G.J. and A.M. Davis (1993) *GCA* 57(1), 231-243. [7] MacPherson G. et al. (1982) *LPSC XIII. 1079-1091*. [8] Simon J.I. et al. (2005) *EPSL*, 38(3-4), 272-283.[9] Kawasaki N. et al. (2016) GCA (*in press*). [10] Needham A. et al. *(2015) 78th Annual Meeting of the Meteoritical Society,* Abstract #5014 [11] Mane P. et al. (2016) *LPSC XLVII*. Abstract #2560. [12] Ito M. and Messenger S. (2008) *71th Annual Meeting of the Meteoritical Society,* Abstract #5100. [13] Simon, J.I., et al., (2016) *GCA* (*in press*). [14] Simon J.I., et al., (2011) *Science*, 331(6021), 1175-8. [15] Keller L. et al. (2013) *76th Annual Meeting of the Meteoritical Society,* Abstract #5300 [16] Wark D. and Boynton W. V. (2001) *MAPS,* 36(8), 1135-1166. [17] Ruzicka A. and Boynton, W. (1991) *Meteoritics*, 26, 39 [18] Zega T. et al. (2016) *LPSC* XLVII, Abstract #2807. [19] Meteoritical Bulletin, no. 103, in preparation (2014). [20] Barber D. et al. (1984) *GCA,* 48(4), 769-783.